

An Improved Multi-Objective Brain Storm Optimization Algorithm for Hybrid Microgrid Dispatch

Kai Zhang, CHN Energy Xinjiangganquanpu Comprehensive Energy Co., Ltd., China*

Zi Tang, CHN Energy Xinjiangganquanpu Comprehensive Energy Co., Ltd., China

ABSTRACT

The increasing integration of renewable energy sources into microgrids has led to challenges in achieving daily optimal scheduling for hybrid alternating current/direct current microgrids (HMGs). To solve the problem, this article presents a novel hybrid AC/DC microgrid scheduling method based on an improved brain storm optimization (BSO) algorithm. Firstly, with economic and energy storage device health as the primary objective functions, this paper proposes a dispatch model for AC-DC hybrid microgrids. To overcome the limitations of traditional algorithms, including premature convergence and can only find non-inferior solution sets, this article proposes a multi-objective BSO algorithm that integrates learning and selection strategies. Additionally, a fuzzy decision-making method is employed to achieve optimal daily dispatching and select the most suitable compromise solution. Finally, experiments are conducted to verify the effectiveness of the proposed multi-objective optimal scheduling method and to demonstrate the practicality and effectiveness of the method in real application scenarios.

KEYWORDS

Alternating Current/Direct Current, Brain Storm Optimization, Fuzzy Decision Making, Microgrid, Multi-objective Optimization

INTRODUCTION

With the increasing demand for electricity, the structure of the power grid is becoming more and more complex, with centralized power generation, large grids for long-distance transmission and other traditional grid structures also facing more challenges, including high costs, difficulty in operation, and difficulty in meeting the user's requirements for high quality, high reliability power and diversified power supply needs. In order to make the power grid run more securely and economically, the smart grid with distributed power supply as the main unit came into being. However, when a power system failure occurs, distributed power supply must immediately withdraw from operation, which limits the role of distributed power supply.

DOI: 10.4018/IJSIR.336530

*Corresponding Author

This article published as an Open Access article distributed under the terms of the Creative Commons Attribution License (<http://creativecommons.org/licenses/by/4.0/>) which permits unrestricted use, distribution, and production in any medium, provided the author of the original work and original publication source are properly credited.

In order to enhance the benefits of distributed power sources, microgrids have emerged. A microgrid is a small-scale power generation and distribution system consisting of distributed power sources, energy storage devices, energy conversion devices, loads, monitoring and protection devices, and the like. Microgrids effectively reduce the impact of photovoltaic (PV) and wind power output uncertainties on the traditional power grid (Das et al., 2022). To enhance microgrid development and leverage the advantages of AC and DC microgrids in managing renewable energy output uncertainties, the concept of AC/DC HMGs has emerged. These hybrids combine the strengths of AC and DC microgrids, offering a flexible energy management approach (Faraji et al., 2022; Zand et al., 2020; Zhang et al., 2018). They can accept both AC and DC energy sources, converting and controlling them through power electronic devices to accommodate various energy inputs (Ansari et al., 2020). As a result, AC and DC renewable energy sources can be seamlessly integrated into the AC/DC HMGs (Heidari et al., 2022; Jayaram et al., 2022).

The increasing penetration of renewable energy sources in AC/DC HMGs poses challenges for energy management (Ansari et al., 2020). Distributed energy storage systems play a vital role in addressing these challenges and find applications in different aspects of AC/DC HMGs (Elgamal et al., 2022). At the micro-power level, these systems can be efficiently scheduled and managed. However, micro-power sources, like photovoltaic generator sets and wind turbines, often exhibit fluctuating power output. Energy storage systems help balance energy supply and demand by storing excess energy for later use or releasing energy when needed to meet load demands. At the electric load level, distributed energy storage systems can be dispatched and managed as well. These systems store power during periods of low load demand and high renewable energy output, releasing power when load demand is high but renewable energy output is low (Gunantara, 2018). This scheduling balances the difference between grid load and supply, reduces pressure on the conventional power system, and enhances overall stability (Marler & Arora, 2004).

The scheduling optimization problem for AC/DC HMGs refers to finding an optimal scheduling strategy to maximize the operational benefits of the microgrids and satisfy the constraints of voltage, power, and security, taking into account the structural and electrical characteristics of the hybrid AC/DC HMGs, the uncertainty of distributed power sources and loads, market tariffs, and operating costs. Both domestic and international scholars have made notable progress in addressing the problem. For instance, Zhang et al. (2022) proposed a day-ahead scheduling algorithm to improve the energy independence, operational reliability, and economy of port microgrids with a two-phase model. Nawaz et al. (2023) introduced a mixed integer quadratic programming method for energy scheduling of islanded multi-microgrids to balance subgrids' supply and demand, reduce battery degradation, and extend cycle life. Shotorbani et al. (2021) developed a multi-objective real-time environmental management system that considers energy costs and life cycle environmental impacts, using the Lyapunov optimization method to optimize the scheduling of distributed energy storage units. Agrawal et al. (2023) modeled the optimal energy flow (ORF) management problem in a hybrid power system containing multiple energy sources and proposed a multi-objective optimization algorithm integrating an innovative nondominated sorting and congestion distance strategy to deal with the ORF problem and improve the reliability of the system. To solve the uncertainty problem in hybrid power systems, a novel hybrid evolutionary algorithm was proposed by Avvari et al. (2023). Zhang et al. (2023) developed an improved NSGA-III algorithm with a dynamic constraint relaxation mechanism and elimination strategy for efficient multi-objective solving.

Although the existing literature has made many contributions to the AC/DC HMGs scheduling problem, there are still some problems, such as a single mathematical model, failure to consider the consumption of the power transmission process, and the fact that only a set of non-inferior solution sets can be found instead of optimal solutions. In order to solve the above problems, we model the AC/DC HMGs scheduling optimization problem by considering the effects of various factors and propose an improved multi-objective BSO algorithm to solve the AC/DC HMGs scheduling optimization problem. The contributions of this paper are as follows:

- 1) Establishing an AC/DC HMGs scheduling model with economic efficiency and energy storage device health as the objective function by deeply studying the impacts of load rate, environment and other factors on AC/DC HMGs.
- 2) Proposing an improved multi-objective BSO algorithm in order to speed up convergence as well as to maintain diversity, a replication operator based on a learning mechanism, a selection operator capable of adaptively balancing convergence and diversity, and since the multi-objective optimization problem ultimately yields a set of solution sets, fuzzy decision-making methods are used in order to select a non-inferior solution.
- 3) Verifying the effectiveness of the proposed multi-objective BSO algorithm based on the data generated from the model.

PRELIMINARIES

Multi-Objective Problem

A multi-objective optimization problem (MOP) means that the problem to be optimized has multiple conflicting objective functions, a minimization multi-objective optimization problem is defined as follows (Caramia et al., 2020; Konak et al., 2006):

$$\begin{aligned} \min F(\mathbf{x}) &= (f_1(\mathbf{x}), f_2(\mathbf{x}), \dots, f_m(\mathbf{x}))^T \\ \text{s.t.} \quad &\begin{cases} g_i(\mathbf{x}) \leq 0, & i = 1, 2, \dots, p \\ h_j(\mathbf{x}) = 0, & j = 1, 2, \dots, q \end{cases} \end{aligned} \quad (1)$$

where $\mathbf{x} \in \mathbb{R}^d$ is a d -dimensional decision vector, $x_i (i = 1, 2, \dots, d)$ is the i -th dimensional decision variable of \mathbf{x} . And $F(\mathbf{x}) \in \mathbb{R}^m$ is an m -dimensional objective vector, $f_i(\mathbf{x})$ is the i -th objective function of $F(\mathbf{x})$. And $g_i(\mathbf{x})$, ($i = 1, 2, \dots, p$) and $h_j(\mathbf{x})$, ($j = 1, 2, \dots, q$) are the p inequality constraints and q equality constraints to be satisfied during the optimization process, respectively.

Definition 1: Pareto dominance and non-dominance. Given two solutions \mathbf{x}^1 and \mathbf{x}^2 , \mathbf{x}^1 is said to dominate \mathbf{x}^2 if $f_i(\mathbf{x}^1) \leq f_i(\mathbf{x}^2)$ for $\forall i \in \{1, 2, \dots, m\}$ and $f_j(\mathbf{x}^1) < f_j(\mathbf{x}^2)$ for $\exists j \in \{1, 2, \dots, m\}$, denoted by $\mathbf{x}^1 \succ \mathbf{x}^2$. \mathbf{x}^1 and \mathbf{x}^2 are said to be non-dominated, if the two solutions do not dominate each other (Deb et al., 2002).

Definition 2: Pareto optimality. $\mathbf{x} \in \Omega$ is referred as a Pareto optimal solution if $\nexists \mathbf{y} \in \Omega$ s.t. $\mathbf{y} \succ \mathbf{x}$ (Murugan et al., 2009).

Brain Storm Optimization

Shi et al. (2013) simulates the process of the brain storm method by utilizing optimization algorithms and proposes the BSO algorithm. The basic idea of the BSO algorithm (Cheng et al., 2016; Ma et al., 2020; Shi, 2011; Shi et al., 2013) is to simulate human thinking activities, find local optimal solutions through the ideology of clustering, obtain the global optimal solution by comparing the local optimal solutions, and maintain the diversity through the operation of mutation. The BSO algorithm's basic process is as follows:

- 1) Population random initialization
- 2) Clustering
- 3) Reproduction

- 4) Mutation
- 5) Environmental selection
- 6) Return to step (2) and continue until the maximum number of evaluations/iterations is reached.

Steps 2, 3 and 4 are the main operations of BSO. In step 3, there are four main ways to generate new individuals by randomly selecting them according to the probability, which are selecting a clustering center, an individual in a class, two clustering centers or two individuals belonging to different classes, and then generating new individuals by weighting them with the current individuals. Then the new generated individuals are mutated by the Gaussian mutation operator in step 4 to prevent from falling into the local optimum, and the Gaussian mutation operator is defined as follows:

$$\mathbf{x}_i^{new} = \mathbf{x}_i + v \times N(\mu, \sigma^2) \quad (2)$$

where \mathbf{x}_i and \mathbf{x}_i^{new} is the i -th dimension of \mathbf{x} and \mathbf{x}^{new} , respectively. $N(\mu, \sigma^2)$ is a Gaussian random function, which μ and σ^2 are the mean and variance. v is a parameter, which is defined below.

$$v = r \times \log \text{sig} \frac{t_{\max} - 2t}{2k} \quad (3)$$

where r is a number between 0 and 1. t_{\max} and t are the maximum iterations and consumed iterations, respectively. $\log \text{sig}(\cdot)$ is a logarithmic sigmoid transfer function and k is a user-defined parameter that controlled the slope of $\log \text{sig}(\cdot)$.

PROBLEM FORMULATIONS

In this section, the general structure of HMG is provided, followed by mathematical modeling of the components of HMG.

Architecture of HMG

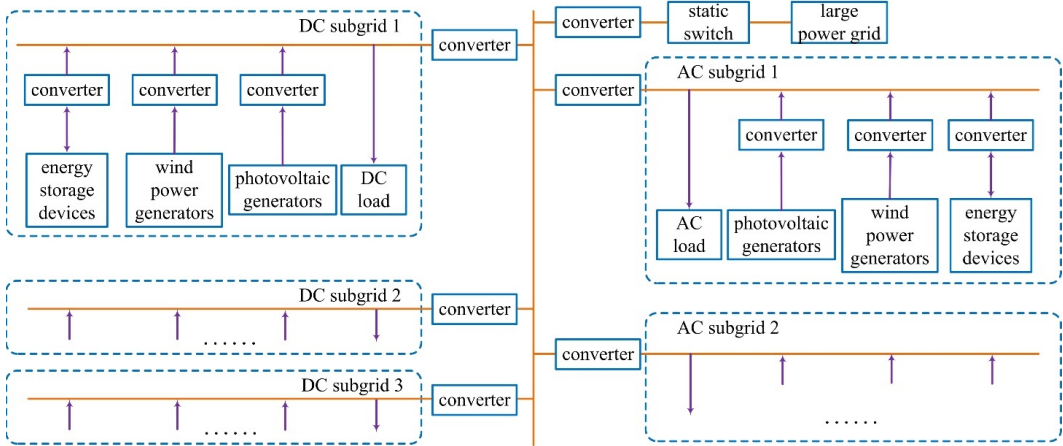
As shown in Figure1, there are multiple DC subgrids and AC subgrids in an AC/DC HMGs, each of which consists of wind power generators, photovoltaic power generators, energy storage devices, local loads, and interface converters connecting the buses to each power source. The connection between the public DC bus and the large power grid is realized through static switches, which in turn accomplishes the power interaction between the AC/DC HMGs and the large power grid.

Distributed Power Model

Wind Power Generator Model

The amount of power generated by a wind turbine depends mainly on the current wind speed. When the wind speed is different, the wind turbine presents three states: cut-out, partial power generation, and full power generation. When the wind speed is greater than the cut-out wind speed v_2 or less than the cut-in wind speed v_1 , the wind turbine cuts out of the grid; when the wind speed is greater than the cut-in wind speed v_1 and less than the rated wind speed v_3 , the wind turbine generates part of the power. In addition, the wind turbine generates full power p'_1 . The power generation of wind turbine P_1 is expressed as follows:

Figure 1. AC/DC HMGs architecture



$$P_1 = \begin{cases} 0 & v < v_1 \text{ or } v > v_2 \\ \frac{v^3 - v_1^3}{v_3^3 - v_1^3} & v_1 \leq v < v_3 \\ p_1' & v_3 \leq v \leq v_2 \end{cases} \quad (4)$$

Photovoltaic Generator Model

Photovoltaic power generation usually increases with the increase of solar light intensity. In addition, the cell surface temperature also has an impact on the power generation. In general, the higher the surface temperature of the cell, the lower its efficiency. High temperatures result in a blockage of electron movement inside the cell, which reduces the output power of the cell. The mathematical model of photovoltaic power generation is defined as follows:

$$P_2 = P_2' \left(\frac{G}{G'} \right) [1 + \alpha(T - T')] \quad (5)$$

where P_2 is the output power of the photovoltaic power generation equipment. P_2' is the rated output power of the photovoltaic power generation equipment. G is the actual solar radiation intensity. G' is the standard solar radiation intensity. T is the actual surface temperature of the photovoltaic power generation. T' is the reference surface temperature of the photovoltaic power generation. α is the power temperature coefficient, which expresses the degree of influence of the change in unit temperature on the output power of the photovoltaic cell.

Energy Storage Device Model

During operation, the state of charge and output power of the energy storage device are modeled as follows:

$$S(t+1) = S(t) + \gamma P_3(t)\delta \quad (6)$$

where $S(t)$ is the state of charge of the energy storage device at the moment t . γ is the charging and discharging efficiency. $P_3(t)$ is the charging and discharging power of the energy storage device at the moment t . When $P_3(t) > 0$, the energy storage device is charged; when $P_3(t) \leq 0$, the energy storage device is discharged. δ is the time interval.

Charging, Discharging, and Power Purchase and Sale

In actual operation, the total power of photovoltaic power generation and wind power generation is not necessarily equal to the electrical load, and the following power difference exists:

$$P_\Delta(t) = P_4(t) - P_1(t) - P_2(t) \quad (7)$$

where $P_\Delta(t)$ is the power difference between the power generated by the wind power generator and the photovoltaic power generator and the electrical load at the moment t , and $P_4(t)$ is the electrical load of the grid at the moment t .

When the power consumption load is not equal to the power generation in the AC/DC HMGs, it is necessary to utilize the energy storage device to balance the system capacity. If the power balance within the grid cannot be realized even through the energy storage device, the power balance will be realized by purchasing and selling power to the grid through the contact line, then there is defined as follows:

$$P_m(t) = P_\Delta(t) + P_3(t) \quad (8)$$

where $P_m(t)$ is the power purchased and sold with the larger grid at moment t . Power is purchased when $P_\Delta(t) > 0$ and sold when $P_\Delta(t) < 0$.

Improved Charging and Discharging Strategies

The charging and discharging strategy of the energy storage device is the key to reduce the operation cost and improve the operation stability of AC/DC HMG. An improved charging and discharging strategy is proposed by considering the charge state of the energy storage device in conjunction with the characteristics of the electricity price during peak and valley hours.

When the electricity price is in the peak hours, the sale of electricity is prioritized to earn revenue. If the power generation of the AC/DC HMG is higher than the local load, the energy storage device discharges as much as possible within the permitted range and sells electricity to the large grid to earn revenue; if the power generation of the AC/DC HMG is lower than the local load, the energy storage device discharges to meet the demand for electricity. When the energy storage device cannot meet the demand, it is necessary to consider purchasing electricity from the grid.

When the electricity price is in the valley, the power purchase strategy should be prioritized. Within the charge state of the energy storage device, power should be purchased from the grid, when the purchased power meets both the charging demand of the energy storage device and the local load gap. When the charge state of the energy storage device reaches the upper limit, energy storage ends. At this time, the purchased power only meets the local load gap.

When the electricity price is in the leveling stage, maintaining the charge state of the energy storage device is prioritized. When the power generation of the AC/DC HMG is higher than the local

load, priority is given to charging the energy storage device, and when the charge state of the energy storage device reaches the upper limit, the charging ends and power is sold to the big grid. When the power generation of the AC/DC HMG is lower than the local load, the energy storage device is prioritized to be dispatched for discharging to maintain the grid operation.

Multi-Objective Optimization Model for AC/DC HMGs

Objective Functions

The economic efficiency of AC/DC HMG and the health degree of energy storage device are taken as the optimization objectives under the premise of guaranteeing the power supply load. The specific objective functions are as follows:

$$\begin{cases} f_1 = \sum_{i=1}^Z \sum_{t=1}^T (s_1 P_1(t) + s_2 P_2(t) + s_3 |P_3(t)|) \delta + \sum_{i=1}^Z \sum_{t=1}^T (c(t) P_{\Delta}(t)) \delta \\ f_2 = e^{-\frac{1}{Z} \sum_{i=1}^Z \sqrt{\frac{1}{T} (\sum_{t=1}^T (S_{net}^i(t) - \bar{S}_{net}^i)^2)}} \end{cases} \quad (9)$$

where f_1 is the operating cost of the AC/DC HMG. f_2 is the magnitude of the change in the state of charge of the energy storage device. Z is the total number of subgrids. T is the total number of time slots. s is the cost of operation per unit of time of the energy storage device. $P_3(t)$ is the charging and discharging power of the energy storage device at the moment of t . δ is the time interval. c is the purchased and sold electricity tariff of the large grid at the moment of t . $P_{\Delta}(t)$ is the sold or purchased power with the large grid at the moment of t . And, \bar{S}_{net}^i is the average state of charge of the energy storage device.

Constraints

The following constraints exist in this AC/DC HMG multi-objective optimization model:

- Power constraint within the subgrids

$$P_{net}^i = P_{net1}^i(t) + P_{net2}^i(t) - P_{net4}^i(t) - P_{net3}^i(t) \quad (10)$$

where P_{net}^i is the output power of the i -th subgrid at the moment t . $P_{net1}^i(t)$ is the photovoltaic power in the i -th subgrid at the moment t . $P_{net2}^i(t)$ is the wind power in the i -th subgrid at the moment t . $P_{net4}^i(t)$ is the charging and discharging power of the energy storage device in the i -th subgrid at the moment t . And, $P_{net3}^i(t)$ is the load consuming power of the i -th subgrid at the moment t .

- Power constraint within the subgrid

$$P_5(t) = \sum_{i=1}^Z P_{net}^i \quad (11)$$

- Energy storage device state-of-charge constraints

$$\begin{cases} S_{net}^1(1) = S_{net}^2(1) = S_{net}^3(1) = \dots = S_{net}^i(1) = \dots = S_{net}^Z(1) \\ S_{net}^1(T) = S_{net}^2(T) = S_{net}^3(T) = \dots = S_{net}^i(T) = \dots = S_{net}^Z(T) \\ S_{min} \leq S_{net}^i(t) \leq S_{max} \end{cases} \quad (12)$$

where $S_{net}^i(1)$ and $S_{net}^i(T)$ are the state of charge of the i -th subnet at the initial and termination moments, respectively. S_{min} and S_{max} are the minimum and maximum charge of the energy storage device, respectively.

- Energy storage device charge/discharge power constraint

$$P_{min} \leq P_{net}^i(t) \leq P_{max} \quad (13)$$

where P_{min} and P_{max} are the minimum and maximum power for charging and discharging the energy storage device, respectively.

Encoding Strategy

AC/DC HMGs scheduling requires simultaneous determination of the charging and discharging power of the energy storage devices in each subgrid in 24 time intervals, which requires the determination of $i \times 24$ decision variables, and therefore a matrix coding approach is used, where the i -th row denotes the charging and discharging power of the energy storage devices in the i -th subgrid, and the j -th column denotes the charging and discharging power of the storage devices of the subgrids in the j -th time interval.

PROPOSED METHOD

Main Framework

Many algorithms have been proposed in recent years to solve MOPs (Narayanan et al., 2023; Ganesh et al., 2023), but compared to other algorithms, BSO has fewer parameters, is able to utilize global as well as local information, and is able to balance convergence and diversity. So we propose an improved multi-objective BSO algorithm to solve the established multi-objective optimization problem. As shown in Figure 2, we first initialize the population and the reference vector (line 2-3 of Algorithm 1). Then the population is divided into elite and ordinary solution sets using the non-dominated sorting method, and then clustered according to the angle between the ordinary solution set and the reference vector (lines 5-6 of Algorithm 1). After clustering, two offspring generation methods are proposed, in order to accelerate the convergence, let the ordinary solution learn from the elite solution to generate new individuals, in order to maintain the diversity, select two boundary solutions in the elite solution, build the direction vector to generate new individuals, and then mutate the newly generated solutions by Gaussian mutation to prevent falling into local optimum (line 7-9 of Algorithm 1). After generating new individuals, unlike the selection mechanism in the BSO algorithm, we mix the offspring and parent individuals, and then adaptively select the good individuals through our proposed selection mechanism (line 11 of Algorithm 1). After obtaining the final population,

we use the fuzzy decision-making method to select an individual as the final scheduling solution (line 13 of Algorithm1).

Reproduction Strategies

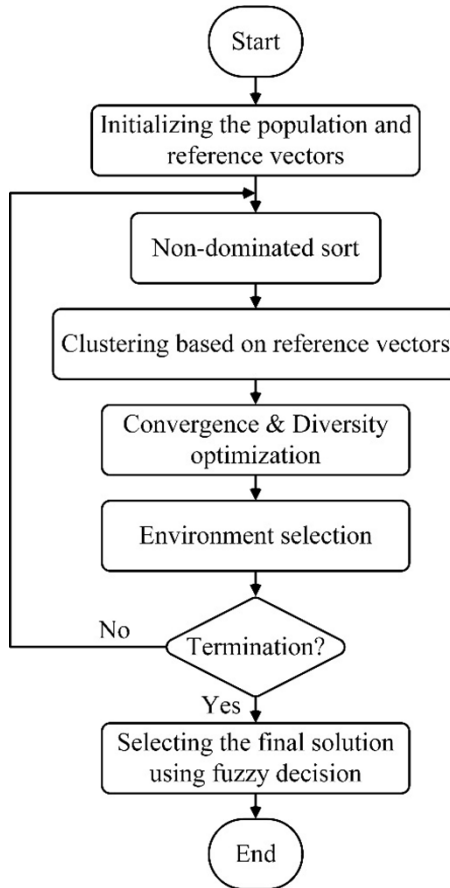
To balance convergence and diversity, we propose two ways of generating individuals. One establishes direction vectors between ordinary and elite solutions to generate convergent individuals (Algorithm 2), and the other establishes direction vectors between elite solutions to generate diverse individuals (Algorithm 3).

For the former, we first divide the current population into nondominated and dominated solution sets by nondominated sorting, take the nondominated solution set as the elite population, and take the dominated solution set as the ordinary population, and then cluster the ordinary population into multiple subpopulations based on the reference vectors; each subpopulation randomly selects an elite solution for learning, and within each subpopulation, builds the direction vectors between the

Algorithm 1. MOBSO

Input: N (Population size), N_{ref} (Reference vectors's number), t_{max} (Maximum iterations)	
Output: X_{best} (Best individual)	
1	$t \leftarrow 0$;
2	$P \leftarrow \text{Initialize_Population}(N)$;
3	$RV \leftarrow \text{Uniform_Reference_Vector}(N_{ref})$;
4	while $t < t_{max}$ do
5	$P_{nd}, P_d \leftarrow \text{NDSort}(P)$;
6	$Clusters \leftarrow \text{Clustering}(P_d, RV)$;
7	$P_{conv} \leftarrow \text{Convergence_Optimization}(P_{nd}, Clusters)$;
8	$P_{div} \leftarrow \text{Diversity_Optimization}(P_{nd})$;
9	$P_{offs} \leftarrow \text{Gaussian_Mutation}(P_{conv}, P_{div})$;
10	$P \leftarrow P \cup P_{offs}$;
11	$P \leftarrow \text{Environment_Selection}()$;
12	end
13	$X_{best} \leftarrow \text{Fuzzy_Decision}(P)$;
14	return X_{best} ;

Figure 2. Flowchart of proposed algorithm



individuals to the elite solutions, and then generates convergent individuals based on equation 14 to generate convergent individuals. For the latter, we randomly select an elite solution, then rank the elite solutions according to a randomly selected objective, select the two elite solutions with the largest and smallest rankings, and then build direction vectors between the two solutions to generate diverse individuals according to equation 15.

$$X_{new} \leftarrow X + r \frac{X_{nd}^r - X}{\|X_{nd}^r - X\|} \quad (14)$$

$$X_{new} \leftarrow X_{nd}^r + r \frac{X_{nd}^r - X_f}{\|X_l - X_f\|} \quad (15)$$

where X_{new} is the newly generated individual, X and X_{nd}^r are the common individual and the randomly selected elite individual, respectively. X_l and X_f are the bounded solutions after sorting according to a certain objective. Following the end of generating the offspring population, the offspring population is mutated using Gaussian mutation (equations (2)-(3)), to prevent falling into a local optimum.

Algorithm 2. Convergence optimization

Input: P_{nd} (Non-dominated solution set), $Clusters$ (Different common subpopulations after clustering)	
Output: P_{conv} (Convergence solution set)	
1	$P_{conv} \leftarrow \emptyset ;$
2	foreach $pop \in Clusters$ do
3	$X_{nd}^r \leftarrow$ random select a non-dominated solution from $P_{nd} ;$
4	foreach $X \in pop$ do
5	$r \leftarrow N(0, 1);$
6	$X_{new} \leftarrow X + r \frac{X_{nd}^r - X}{X_{nd}^r - X} ;$
7	$P_{conv} \leftarrow \{ P_{conv}, X_{new} \};$
8	end
9	end
10	return $P_{conv} ;$

Environment Selection Strategy

In order to retain individuals with different characteristics at different stages, we propose an adaptive offspring selection mechanism (Algorithm 4). Specifically, the offspring population and the parent population are first mixed together, using the Euclidean distance of individuals to the ideal point as a criterion for judging convergence, using the aggregation distance as a criterion for judging diversity, and combining the two to form an adaptive selection metric as follows:

$$m \leftarrow \ln \left(\frac{t_{max}}{t} \times \frac{AD}{ED} \right) \tag{16}$$

where t and t_{max} are the current iterations and the maximum iterations, respectively. AD and ED are the aggregation distance of the individual and the Euclidean distance of the individual to the ideal point, respectively. After calculating the metrics of all individuals in the population, the metrics are sorted according to the metrics, and the top N individuals are selected as the new population after sorting. With the proposed metric, it is possible to select individuals with good convergence in the early stage and good diversity in the later stage.

Algorithm 3. Diversity optimization

Input: P_{nd} (Non-dominated solution set)	
Output: P_{div} (Diversity solution set)	
1	$P_{div} \leftarrow \emptyset$;
2	$N_{nd} \leftarrow \text{Size}(P_{nd})$;
3	$i \leftarrow 1$;
4	for $i \leq N_{nd}$ do
5	Sort_By_Any_Objective(P_{nd});
6	$[X_f, X_l] \leftarrow [P_{nd}(1), P_{nd}(N_{nd})]$;
7	$X_{nd}^r \leftarrow$ random select a non-dominated solution from P_{nd} ;
8	$r \leftarrow N(0, 1)$;
9	$X_{new} \leftarrow X_{nd}^r + r \frac{X_{nd}^r - X_f}{X_l - X_f} ;$
10	$P_{div} \leftarrow \{P_{div}, X_{new}\}$;
12	end
13	return P_{div} ;

Fuzzy Decision Strategy

After obtaining multiple candidate scheduling solutions, this paper uses a fuzzy decision-based strategy to select the best scheduling solution. Fuzzy decision-making is a decision analysis method based on fuzzy theory (Han et al., 2022; Hussain et al., 2019; Ishraque et al., 2021; Ma et al., 2020; Ting et al., 2015). Unlike traditional decision-making methods, it does not require explicit weight relationship relations between objectives but uses fuzzy facts and fuzzy rules to describe the uncertainty and inaccuracy existing in the decision-making process. First, the membership function of the i -th objective of the k -th scheduling solution is defined as follows:

Algorithm 4. Environment selection

Input: P (Solution set), t (Current iterations), t_{max} (Maximum iterations), N (Population size)	
Output: $P_{survival}$ (Survival solution set)	
1	$P_{survival} \leftarrow \emptyset$;
2	$Z^* \leftarrow$ Ideal Point (P);
3	$M \leftarrow \emptyset$;
4	for $i \leq N_{nd}$ do
5	$ED \leftarrow$ Compute Euclidean Distance (Z^*, x);
6	$AD \leftarrow$ Compute Euclidean Distance (P, x);
7	$m \leftarrow \ln \left(\frac{t_{max}}{t} \times \frac{AD}{ED} \right)$;
8	$M \leftarrow \{M, m\}$;
9	end
10	$[\sim, index] \leftarrow$ Sort (M', Asc');
11	$P_{survival} \leftarrow P$ (index (1:N));
12	return $P_{survival}$;

$$\mu_i^k = \begin{cases} 1 & f \leq f_i^{\min} \\ \frac{f_i^{\max} - f_i}{f_i^{\max} - f_i^{\min}} & f_i^{\min} < f_i < f_i^{\max} \\ 0 & f_i^{\max} \leq f_i \end{cases} \quad (17)$$

where f_i^{\min} and f_i^{\max} are the minimum and maximum values of the i -th objective function. The larger the value of the membership function of the scheduling solution on the objective, the higher the satisfaction of the objective.

For the k -th candidate scheduling solution, compute the normalized membership function value as follows:

$$\mu^k = \frac{\sum_{i=1}^3 \mu_i^k}{\sum_{k=1}^M \sum_{i=1}^3 \mu_i^k} \quad (18)$$

where N is the number of candidate scheduling solutions and N_{obj} is the number of objectives.

SIMULATION EXPERIMENT AND RESULT ANALYSIS

Parameter Settings

In this paper, a multi-subgrid AC/DC HMGs model is constructed, which contains 2 AC subgrids and 3 DC subgrids, and the parameters of each subgrid are the same (see Table 1). The parameters of wind power generation devices, photovoltaic power generation devices and energy storage devices in each subgrid are the same, as shown in Table 1. This experiment adopts the time-sharing tariff mechanism, and the purchased and sold tariffs of each time period are shown in Table 2.

In order to validate the effectiveness of the proposed method, it is compared and analyzed with MOPSO (Yang et al., 2009; Vikram et al., 2021; Ganesh et al., 2021), MOABC (Nasiraghdam & Jadid, 2012), and NSGAI (Deb et al., 2002; Murugan et al., 2009; Joshi et al., 2021). The parameters of the proposed algorithm are set as follows: the population size is 100 and the number of reference vectors is 10. The other comparison algorithms follow the parameter settings in the original paper except that the population size is set to 100. In order to compare the different algorithms in a fair way, the number of iterations is used as the termination condition, which is set to 1000. In addition, each algorithm is repeated 10 times on each test case.

Table 1. Parameters of distributed power generation

Devices	Installed power (kW)	Installation cost (/10K CNY • kW-1)	Operation and maintenance factor	Service life
Wind turbines	100	1.37	0.0296	20
Photovoltaic power generation device	80	0.95	0.0096	20
Storage battery	100	2.37	0.045	10

Table 2. Details of the tariffs for each time period

Project	Time interval	Electricity purchase price (/1 CNY • kW-1)	Electricity sales price (/1 CNY • kW-1)
Peak hours	07:00–11:00	0.83	0.65
	17:00–21:00		
Normal hours	05:00–07:00	0.49	0.38
	11:00–17:00		
	21:00–22:00		
Valley hours	00:00–05:00	0.17	0.13
	22:00–24:00		

Table 3. Comparison of the four algorithms

Number of runs	Our Method		MOPSO		MOABC		NSGAI	
	Operating costs	Device Health						
1	487	0.3315	473	0.38154	476	0.4714	486	0.397
2	483	0.3313	461	0.5345	476	0.6827	486	0.4005
3	488	0.2351	494	0.208	474	0.5183	485	0.1874
4	479	0.4444	481	0.3669	470	0.3347	487	0.1171
5	487	0.2974	483	0.2128	491	0.3094	488	0.3031
6	461	0.2738	491	0.6307	503	0.4168	490	0.3222
7	487	0.3028	463	0.7098	506	0.3958	496	0.5576
8	462	0.3127	476	0.3455	497	0.3517	496	0.7699
9	484	0.364	499	0.5799	475	0.4908	491	0.7551
10	454	0.3686	495	0.3059	502	0.6198	492	0.4205
Avg	477.2	0.3261	481.6	0.4275	487	0.4591	489.7	0.4230
Std	12.3	0.0546	12.6	0.1665	13.4	0.1164	3.8	0.2058

Table 4. Mean and standard deviation results for HV after ten independent runs of the four algorithms

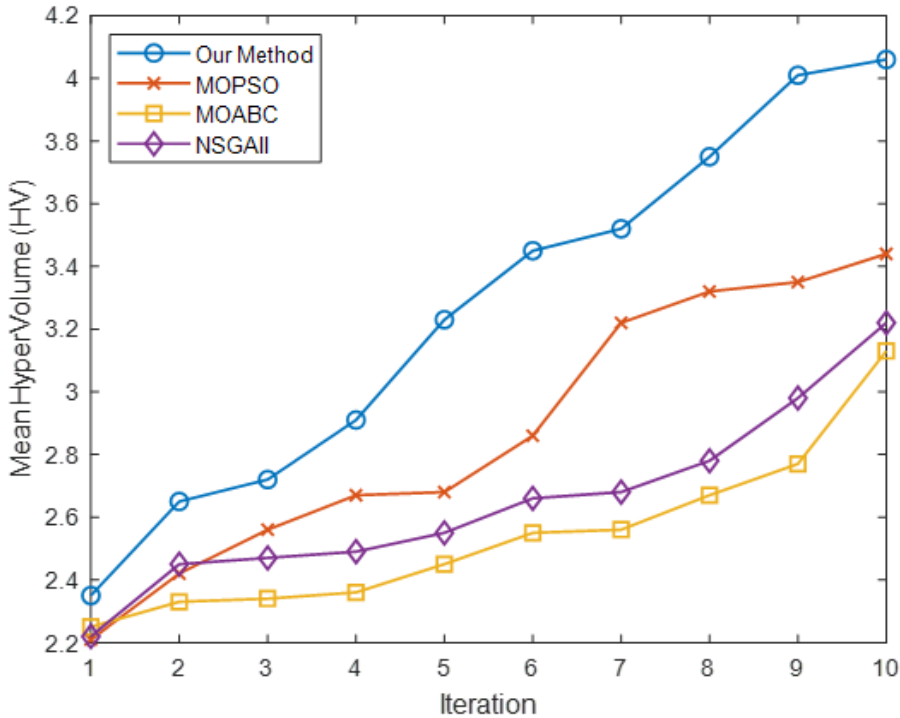
Our Method	MOPSO	MOABC	NSGAI
4.06e+0(1.90e-1)	3.44e+0(2.35e+0)+	3.13e+0(1.21e-1)+	3.22e+0(1.56e+0)+

DISCUSSION AND ANALYSIS

Wilcoxon’s rank sum test at a 0.05 significance level is performed between REA-HC and each compared algorithm. +, - and \approx denote that our method is significantly better than, significantly worse than or not significantly different from its compared algorithm, respectively.

The objective values obtained under 10 independent runs are shown in Table 3. Comparing MOPSO, MOABC and the algorithm proposed in this paper, it can be found that the standard deviation of the optimization objective obtained by the algorithm proposed in this paper in the test cases is smaller, which indicates that our proposed strategy has a significant effect on improving the stability of the algorithm, and it can effectively avoid the problems of premature convergence and the tendency to fall into local optimum. In addition, NSGAI has the weakest algorithmic performance, and the average values of the optimization objectives in the test cases all have a large gap with the other algorithms. However, the stability of its algorithm is better, indicating that the environment selection strategy based on congestion distance has a certain effect on maintaining the stability of the algorithm. In addition, we also used hypervolume (HV) as a performance metric and performed Wilcoxon rank sum test at 0.05 level of significance, and the results obtained are shown in Table 4, where our proposed algorithm is strongest among all the algorithms, which indicates that the overall performance of our method is significantly better than the other comparative algorithms. The relationship between the average HV value of the 10 independent runs and the number of iterations is shown in Figure 3, which indicates that the convergence of our proposed algorithm is better than the other algorithms. The algorithm proposed in this paper is generally better than the other three

Figure 3. Mean HV values with the number of iterations under ten independent runs



algorithms, which verifies the effectiveness of the reproduction strategies and selection strategy proposed in this paper.

The optimal multi-objective scheduling solution obtained by the algorithm proposed in this paper is shown in Figures 4 and 5. In the valley period 1 (00:00-05:00) and the usual period 1 (05:00-07:00), the subgrid PV is basically not out of power, and the wind power generation cannot meet the demand for electricity. At this time, the electricity price is low, and the battery charge state is in the middle, so priority is given to maintaining the battery charge state. Each sub-grid purchases power from the grid at the same time to share the power deficit and charge the batteries after meeting the load demand. During peak hour 1 (07:00-11:00), PV power generation gradually increases, and the wind power output in each subgrid is close to the power demand. At this time, the electricity price is higher, and the battery discharging strategy is prioritized. Battery discharge and PV, wind power together to meet the demand for electricity, while selling electricity to the grid to earn revenue. In the usual period 2 (11:00-17:00), PV power generation reaches its peak, and the wind power in each subgrid is higher than the electricity demand. At this time, the price of electricity is in the middle, and the strategy of maintaining the battery charge state is prioritized. The batteries in each subgrid are turned into charging state, and the purchased power meets the load power difference and battery charging demand, so as to ensure that the batteries have sufficient reserve power in the next peak hour. In peak hour 2 (17:00-21:00), the PV power gradually decreases to 0, and the wind power gradually fails to meet the power demand. At this time, the price of electricity is higher, and the battery after the usual period of charging, the charge state maintains a high level, prioritize the discharge strategy. The battery is discharged to meet the demand for electricity, and at the same time, a small amount of electricity is sold to the grid to earn revenue. In valley time 2 (22:00-24:00), the wind power cannot

Figure 4. Electricity purchase and sale of each subnet

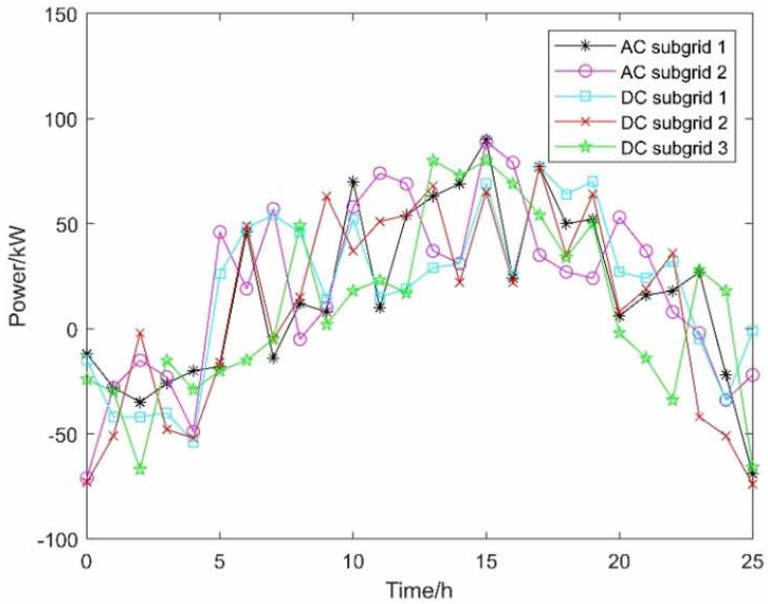
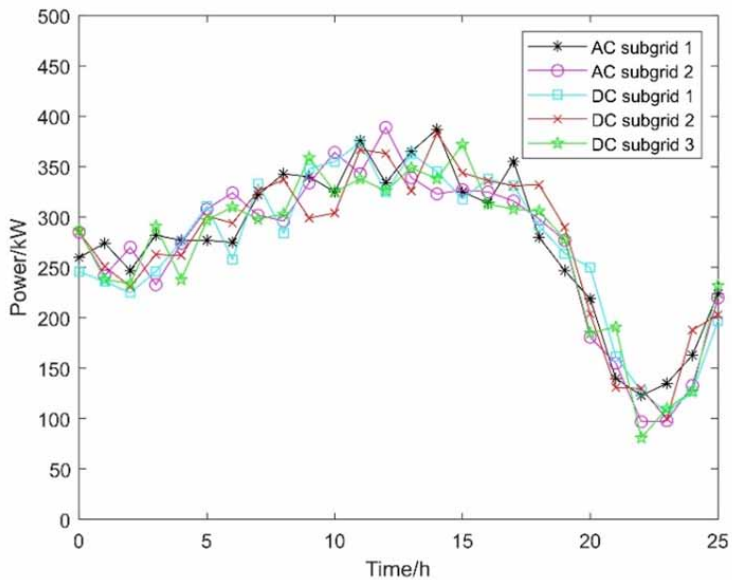


Figure 5. State of charge of energy storage equipment of each subnet



meet the demand for electricity. At this time, the electricity price is low, and the power purchase strategy is prioritized. Since the battery charge state of DC subgrid 2 is slightly higher than the initial state, it can continue to be discharged; while the battery charge state of DC subgrid 1 and AC subgrid 1 is lower than the initial state, in order to maintain the battery charge state equal at the beginning and

the end, the purchased power needs to satisfy the electricity load and battery charging demand at the same time.

In the future, we consider combining deep learning models (Kalita et al., 2021; Dey et al., 2023) and genetic algorithms to improve the execution efficiency of the algorithms by utilizing the data-driven nature of deep learning to predict the data in the microgrid, and then using the predicted values and the prediction error as the selection criteria.

CONCLUSION

Taking into consideration the operational characteristics of the AC/DC HMGs system, along with real-time electricity prices and the charge status of the energy storage devices, a scheduling model for the AC/DC HMGs is formulated. This model aims to optimize both the economic benefits and the health of the energy storage devices, utilizing an improved multi-objective brain storm optimization (BSO) algorithm based on learning and selection strategies. Additionally, a fuzzy decision-making approach is implemented to identify the optimal compromise solution. The analysis of energy storage device outputs during peak hours, valley hours, and flat hours leads to the following conclusions.

The proposed algorithm effectively addresses the limitations of traditional algorithms, avoiding premature convergence and providing a non-inferior solution set. Comparative experiments with other multi-objective algorithms validate the effectiveness of the proposed approach. Moreover, the simulation results align well with real-world situations and can be applied to regulate the output of each unit in real-time.

The hybrid AC/DC microgrid scheduling method based on the improved BSO algorithm significantly enhances economic efficiency and ensures the health of energy storage devices. Detailed analysis of experimental results demonstrates its ability to dynamically adapt to load variations, optimizing operating costs, and improving overall system power quality. As a result, this method offers a flexible and effective solution for enhancing the performance and sustainability of AC/DC HMGs.

REFERENCES

- Agrawal, S., Pandya, S., Jangir, P., Kalita, K., & Chakraborty, S. (2023). A multi-objective thermal exchange optimization model for solving optimal power flow problems in hybrid power systems. *Decision Analytics Journal*, 8, 100299. doi:10.1016/j.dajour.2023.100299
- Ansari, S., Chandel, A., & Tariq, M. (2020). A comprehensive review on power converters control and control strategies of AC/DC microgrid. *IEEE Access : Practical Innovations, Open Solutions*, 9, 17998–18015. doi:10.1109/ACCESS.2020.3020035
- Avvari, R. K., & DM, V. K. (2023). A novel hybrid multi-objective evolutionary algorithm for optimal power flow in wind, PV, and PEV systems. *Journal of Operation and Automation in Power Engineering*, 11(2), 130–143.
- Caramia, M., & Dell’Olmo, P. (2020). Multi-objective optimization. *Multi-objective management in freight logistics: Increasing capacity, service level, sustainability, and safety with optimization algorithms*, 21–51.
- Cheng, S., Qin, Q., Chen, J., & Shi, Y. (2016). Brain storm optimization algorithm: A review. *Artificial Intelligence Review*, 46(4), 445–458. doi:10.1007/s10462-016-9471-0
- Das, A., Wu, D., & Ni, Z. (2022). Approximate dynamic programming with policy-based exploration for microgrid dispatch under uncertainties. *International Journal of Electrical Power & Energy Systems*, 142, 108359. doi:10.1016/j.ijepes.2022.108359
- Deb, K., Pratap, A., Agarwal, S., & Meyarivan, T. (2002). A fast and elitist multiobjective genetic algorithm: NSGA-II. *IEEE Transactions on Evolutionary Computation*, 6(2), 182–197. doi:10.1109/4235.996017
- Dey, K., Kalita, K., & Chakraborty, S. (2023). A comparative analysis on metamodel-based predictive modeling of electrical discharge machining processes. [IJIDeM]. *International Journal on Interactive Design and Manufacturing*, 17(1), 385–406. doi:10.1007/s12008-022-00939-5
- Elgamal, M., Korovkin, N., Menaem, A. A., & Elmitwally, A. (2022). Day-ahead complex power scheduling in a reconfigurable hybrid-energy islanded microgrid with responsive demand considering uncertainty and different load models. *Applied Energy*, 309, 118416. doi:10.1016/j.apenergy.2021.118416
- Faraji, H., Nosratabadi, S. M., & Hemmati, R. (2022). AC unbalanced and DC load management in multi-bus residential microgrid integrated with hybrid capacity resources. *Energy*, 252, 124070. doi:10.1016/j.energy.2022.124070
- Ganesh, N., Ragavendran, U., Kalita, K., Jain, P., & Gao, X. Z. (2021). Multi-objective high-fidelity optimization using NSGA-III and MO-RPSOLC. *CMES-Computer Modeling in Engineering & Sciences*, 129(2).
- Ganesh, N., Shankar, R., Kalita, K., Jangir, P., Oliva, D., & Pérez-Cisneros, M. (2023). A novel decomposition-based multi-objective symbiotic organism search optimization algorithm. *Mathematics*, 11(8), 1898. doi:10.3390/math11081898
- Gunantara, N. (2018). A review of multi-objective optimization: Methods and its applications. *Cogent Engineering*, 5(1), 1502242. doi:10.1080/23311916.2018.1502242
- Han, D., Du, W., Jin, Y., Du, W., & Yu, G. (2022). A fuzzy constraint handling technique for decomposition-based constrained multi-and many-objective optimization. *Information Sciences*, 597, 318–340. doi:10.1016/j.ins.2022.03.030
- Heidari, S., Hatami, A., & Eskandari, M. (2022). An intelligent capacity management system for interface converter in AC-DC hybrid microgrids. *Applied Energy*, 316, 119112. doi:10.1016/j.apenergy.2022.119112
- Hussain, K., Mohd Salleh, M. N., Cheng, S., & Shi, Y. (2019). Metaheuristic research: A comprehensive survey. *Artificial Intelligence Review*, 52(4), 2191–2233. doi:10.1007/s10462-017-9605-z
- Ishraque, M. F., Shezan, S. A., Ali, M., & Rashid, M. (2021). Optimization of load dispatch strategies for an islanded microgrid connected with renewable energy sources. *Applied Energy*, 292, 116879. doi:10.1016/j.apenergy.2021.116879
- Jayaram, J., Srinivasan, M., Prabakaran, N., & Senjyu, T. (2022). Design of decentralized hybrid microgrid integrating multiple renewable energy sources with power quality improvement. *Sustainability (Basel)*, 14(13), 7777. doi:10.3390/su14137777

- Joshi, M., Ghadai, R. K., Madhu, S., Kalita, K., & Gao, X. Z. (2021). Comparison of NSGA-II, MOALO and MODA for multi-objective optimization of micro-machining processes. *Materials (Basel)*, *14*(17), 5109. doi:10.3390/ma14175109 PMID:34501205
- Kalita, K., Chakraborty, S., Madhu, S., Ramachandran, M., & Gao, X. Z. (2021). Performance analysis of radial basis function metamodells for predictive modelling of laminated composites. *Materials (Basel)*, *14*(12), 3306. doi:10.3390/ma14123306 PMID:34203794
- Konak, A., Coit, D. W., & Smith, A. E. (2006). Multi-objective optimization using genetic algorithms: A tutorial. *Reliability Engineering & System Safety*, *91*(9), 992–1007. doi:10.1016/j.res.2005.11.018
- Ma, L., Cheng, S., & Shi, Y. (2020). Enhancing learning efficiency of brain storm optimization via orthogonal learning design. *IEEE Transactions on Systems, Man, and Cybernetics. Systems*, *51*(11), 6723–6742. doi:10.1109/TSMC.2020.2963943
- Marler, R. T., & Arora, J. S. (2004). Survey of multi-objective optimization methods for engineering. *Structural and Multidisciplinary Optimization*, *26*(6), 369–395. doi:10.1007/s00158-003-0368-6
- Murugan, P., Kannan, S., & Baskar, S. (2009). NSGA-II algorithm for multi-objective generation expansion planning problem. *Electric Power Systems Research*, *79*(4), 622–628. doi:10.1016/j.epr.2008.09.011
- Narayanan, R. C., Ganesh, N., Čep, R., Jangir, P., Chohan, J. S., & Kalita, K. (2023). A novel many-objective sine–cosine algorithm (MaOSCA) for engineering applications. *Mathematics*, *11*(10), 2301. doi:10.3390/math11102301
- Nasiraghdam, H., & Jadid, S. (2012). Optimal hybrid PV/WT/FC sizing and distribution system reconfiguration using multi-objective artificial bee colony (MOABC) algorithm. *Solar Energy*, *86*(10), 3057–3071. doi:10.1016/j.solener.2012.07.014
- Nawaz, A., Wu, J., Ye, J., Dong, Y., & Long, C. (2023). Distributed MPC-based energy scheduling for islanded multi-microgrid considering battery degradation and cyclic life deterioration. *Applied Energy*, *329*, 120168. doi:10.1016/j.apenergy.2022.120168
- Shi, Y. (2011, June 12-15). *Brain storm optimization algorithm*. [Proceedings]. Advances in Swarm Intelligence: Second International Conference, ICSI 2011, Chongqing, China.
- Shi, Y., Xue, J., & Wu, Y. (2013). Multi-objective optimization based on brain storm optimization algorithm. [IJSIR]. *International Journal of Swarm Intelligence Research*, *4*(3), 1–21. doi:10.4018/ijrir.2013070101
- Shotorbani, A. M., Zeinal-Kheiri, S., Chhipi-Shrestha, G., Mohammadi-Ivatloo, B., Sadiq, R., & Hewage, K. (2021). Enhanced real-time scheduling algorithm for energy management in a renewable-integrated microgrid. *Applied Energy*, *304*, 117658. doi:10.1016/j.apenergy.2021.117658
- Ting, T., Yang, X.-S., Cheng, S., & Huang, K. (2015). Hybrid metaheuristic algorithms: Past, present, and future. *Recent advances in swarm intelligence and evolutionary computation*, 71–83.
- Vikram, K., Ragavendran, U., Kalita, K., Ghadai, R. K., & Gao, X. Z. (2021). Hybrid metamodel-NSGA-III-EDAS based optimal design of thin film coatings. *Computers, Materials & Continua*, *66*(2), 1771–1784. doi:10.32604/cmc.2020.013946
- Yang, J., Zhou, J., Liu, L., & Li, Y. (2009). A novel strategy of pareto-optimal solution searching in multi-objective particle swarm optimization (MOPSO). *Computers & Mathematics with Applications (Oxford, England)*, *57*(11-12), 1995–2000. doi:10.1016/j.camwa.2008.10.009
- Zand, M., Nasab, M. A., Sanjeevikumar, P., Maroti, P. K., & Holm-Nielsen, J. B. (2020). Energy management strategy for solid-state transformer-based solar charging station for electric vehicles in smart grids. *IET Renewable Power Generation*, *14*(18), 3843–3852. doi:10.1049/iet-rpg.2020.0399
- Zhang, J., Cai, J., Zhang, H., & Chen, T. (2023). NSGA-III integrating eliminating strategy and dynamic constraint relaxation mechanism to solve many-objective optimal power flow problem. *Applied Soft Computing*, *146*, 110612. doi:10.1016/j.asoc.2023.110612
- Zhang, R., Cheng, X., & Yang, L. (2018). Flexible energy management protocol for cooperative EV-to-EV charging. *IEEE Transactions on Intelligent Transportation Systems*, *20*(1), 172–184. doi:10.1109/TITS.2018.2807184

Zhang, Y., Liang, C., Shi, J., Lim, G., & Wu, Y. (2022). Optimal port microgrid scheduling incorporating onshore power supply and berth allocation under uncertainty. *Applied Energy*, 313, 118856. 唐梓 1989.12.10 男 汉族 四川广安 国能新疆甘泉堡综合能源有限公司 大学本科 工程师 研究光伏、增量配电网、风电等新能源方向